Star Sapphire Doublets

Saengthip Saengbuangamlam and Pimtida Bupparenoo

The Gem and Jewelry Institute of Thailand (Public Organization), Bangkok 10500, Thailand
ssaengthip@git.or.th

Introduction

Asterism or star effect is one of the phenomena found in many gemstones such as corundum, quartz and garnet. The phenomenon is caused by the reflection of light from dense fine needle-like inclusions oriented along with crystallographic structure (commonly two or three directions). High-quality star stones are considered rare and can gain high market values. Hence imitation star stones occasionally appear on the market. Recently, GIT Gem Testing Laboratory (GIT-GTL) has examined three unusual star sapphire doublets shown in Figure 1.

Figure 1 : Three unusual star sapphire doublets weighing 4.43 ct (pinkish-red, left), 3.56 ct (blue, middle) and 2.16 ct (yellow, right), each has a synthetic corundum dome top and a natural star sapphire base. Photo by C. Kamemakanon

Samples and methods

All three samples were semi-translucent oval-shaped cabochons weighing 4.43 ct (pinkish-red), 3.59 ct (blue) and 2.16 ct (yellow) with distinct six-rayed star effect shown in figure 1 from left to right, respectively.

Standard gem testing instruments were used to obtain the gemological properties. External and internal features were observed with a high magnification gemological microscope and fluorescence effects of the stones were observed using standard ultraviolet lamps, long-wave (LWUV, 365 nm) and short-wave (SWUV, 254 nm).

The Raman spectra were collected with a Renishaw inVia spectrometer using 532 nm laser excitation in the range 200–1500 Raman shift (cm^{-1}). X-radiography was performed with a Softex SFX-100 instrument. Chemical compositions were collected with EDXRF Eagle II. The Mid-Infrared (IR) spectral (4000-500 cm^{-1}) features of the stones were collected by a Thermo Nicolet 6700 Fourier-Transform Infrared (FTIR) spectrometer. The Ultraviolet-Visible-Near Infrared (UV-Vis-NIR) spectra were recorded by a PerkinElmer Lambda 1050 spectrophotometer in the range 300-1000 nm.

Gemological properties

All samples showed similar refractive indices (RI) of ~1.76 (spot reading) and specific gravity (SG) values of 3.98-4.05 that are typical for corundum. The pinkish-red stone fluoresced moderately chalky orange in SWUV but was inert in LWUV, the blue stone displayed a chalky blue along curved striations in SWUV and was inert in LWUV, while the yellow stone exhibited very weak red in both SWUV and LWUV (Figure 2a – 2f).

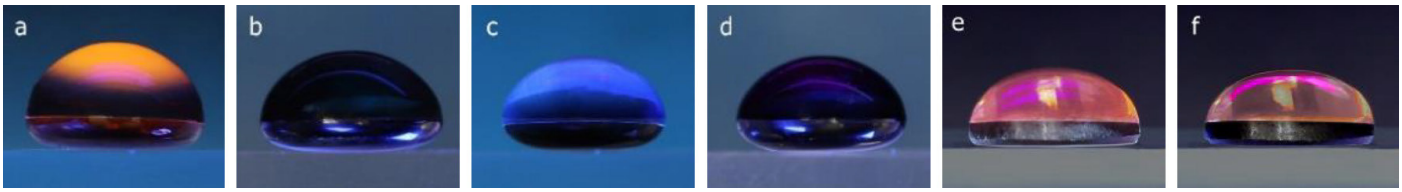

Figure 2 : Fluorescent effect of the pinkish-red sample: chalky orange in SWUV (a) and inert in LWUV (b); the blue sample: chalky blue in SWUV (c) and inert in LWUV (d); the yellow sample: very weak red in both SWUV (e) and LWUV (f).

General and Microscopic features

When observed with naked eye, loupe and microscope, all three stones revealed the character of a composite material consisting of two distinctly different pieces, or doublet: the dome top is a transparent piece of synthetic corundum firmly attached to a natural black star sapphire base. The contact plane can easily be observed from the side view slightly below the stone's girdle (Figure 3a, 3b and 3c).

Further examination showed dense fine silk inclusions along straight and angular growth zones in the base part (Figure 4a, b, c) where the star effect originated. In contrast, many internal inclusions such as tiny gas bubbles, curved striation, or curved color banding can be seen in the dome pieces that confirmed the synthetic origin (Figures 5a,b,c and 6a,b). Furthermore, many flattened trapped gas bubbles can be seen along the contact plane where the two pieces were glued together (Figure 7).

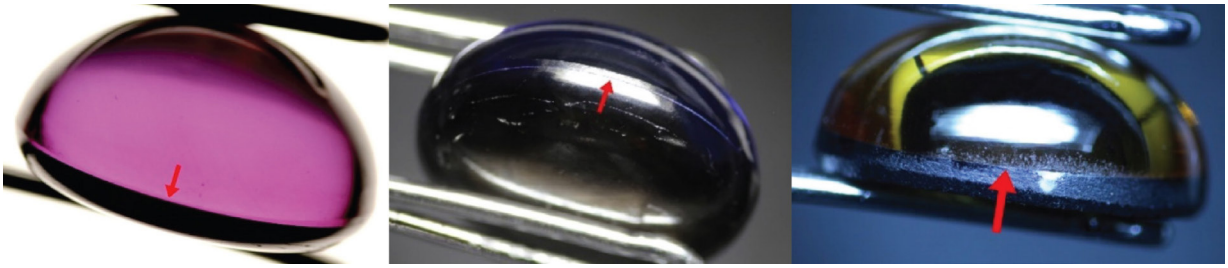

(a) (Magnified 12.5x) (b) (Magnified 12.5x) (c) (Magnified 16x)

Figure 3 : A contact layer where the dome and base pieces of the samples joined together is clearly seen in reflected light (a, c), transmitted diffused light (b).

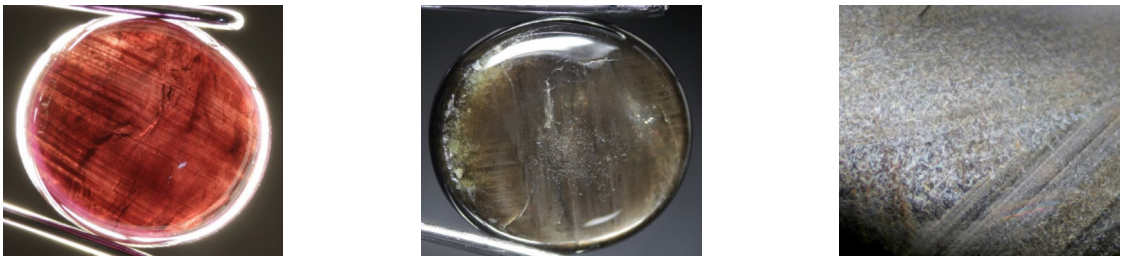

(a) (Magnified 8x) (b) (Magnified 8x) (c) (Magnified 50x)

Figure 4 : Abundant fine silk inclusions when observed under the microscope on the base pieces of pinkish-red sample.

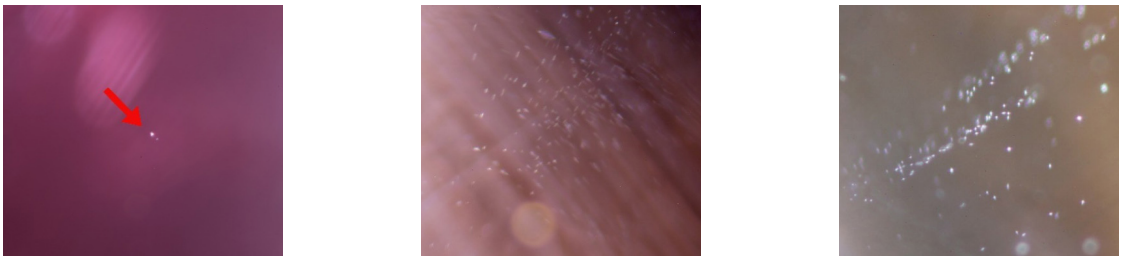

(a) (Magnified 50x) (b) (Magnified 50x) (c) (Magnified 50x)

Figure 5 : Irregularly distributed gas bubbles seeing in the dome pieces of pinkish-red sample (a, b) and blue sample (c), under fiber optic light.

(a) (Magnified 50x) (b) (Magnified 50x)

Figure 6 : Curved growth lines are observed in the dome part of pinkish-red sample (a) and blue sample (b) under diffused light.

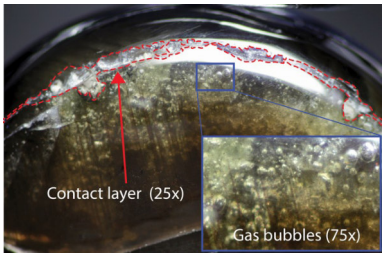

Figure 7 : A lot of large gas bubbles trapped along the contact layer where the two pieces glued together in the pinkish-red sample, reflected light (Magnified 75x)

Advanced Spectroscopic Analyses

Laser Raman spectroscopic analysis

The exposed adhesive substance at the contact plane was identified by Raman spectroscopy to be a type of polymer (Figure 8).

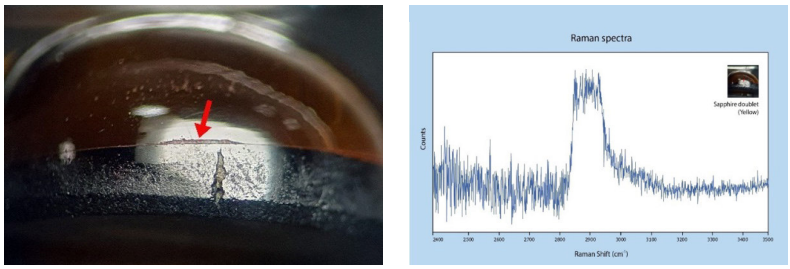

Figure 8 : A close-up view of the contact layer of the dome and base pieces of the yellow sapphire doublet revealed colorless material (left photo, magnified 30x, fiber optic light,) which was identified as a type of polymer (see Raman spectrum on the right diagram).

Chemical analysis

The semi-quantitative chemical analysis of the stones was collected on both dome and base parts. The dome parts of all three stones are composed mainly of Al with traces of Ti, V, Cr, and Fe without Ga (bdl level) that strongly indicate the synthetic corundum. It is noteworthy that the dome part of the pinkish-red sample only contains significant contents of V and Cr which are the most likely cause of the stone's pinkish-red coloration, while the dome part of the blue sample contains significant amounts of Fe and Ti that possibly cause the blue coloration. In contrast, the dome part of the yellow sample contains significant Fe and some Ni contents that probably relate to the stone's yellow coloration. In contrast, the base sides of all three stones comprise mainly Al and significant amounts of Fe, Ti and Ga that are consistent with a natural black star sapphire chemical data. Furthermore, Pb and Si were also detected from the glassy material in fractures of the base part of the pinkish-red sample, suggesting an additional lead-glass fracture-filled treatment.

Table 1 : The chemical analyses of the pinkish-red, blue and yellow sample by EDXRF

Element Oxides (wt.%)	Al_2O_3	TiO_2	V_2O_5	Cr_2O_3	Fe_2O_3	Ga_2O_3	PbO_2	SiO_2	Ni_2O_3
Pinkish- red sample									
- Dome part	99.718	0.007	**0.256**	**0.016**	0.003	bdl	-	-	-
- Base part	98.719	**0.028**	0.005	0.002	**1.222**	**0.024**	-	-	-
- Glassy material in fracture of the base part	87.644	**0.019**	0.003	0.001	**1.705**	**0.027**	**7.705**	**2.986**	-
Blue Sample									
- Dome part	99.948	**0.010**	0.008	0.003	**0.024**	0.007	-	-	-
- Base part	98.722	**0.016**	0.002	0.004	**1.233**	**0.023**	-	-	-
Yellow sample									
- Dome part	99.954	0.010	0.010	0.011	**0.011**	0.002	-	-	**0.002**
- Base part	97.833	**0.051**	0.006	0.028	**2.049**	0.034	-	-	-

bdl = below detection limit

X-radiography

The X-ray images (Figure 9) showed a high-density (dark) zone at the base of the pinkish-red sample while none was found in the blue and yellow samples. This high density zone is consistent with the presence of Pb in the glassy material in fractures of the base part of the pinkish-red sample that suggests a lead-containing glass filler (Promwongnan *et al*., 2016).

Figure 9 : Comparing X-radiographs, the pinkish-red sample (left) shows a high density (dark) zone while the blue (middle) and yellow (right) samples show nothing.

Mid-Infrared spectroscopic analysis

The mid-IR spectrum of the dome part in the pinkish-red stone showed interesting absorption peaks at 3232 cm^{-1} stronger than 3309 cm^{-1} commonly seen in flame-fusion synthetic corundum (Smith, 1995), while the blue sample displayed absorption peaks at 3309 cm^{-1} stronger than 3232 cm^{-1}, and the yellow sample showed no such absorption features (Figure 10).

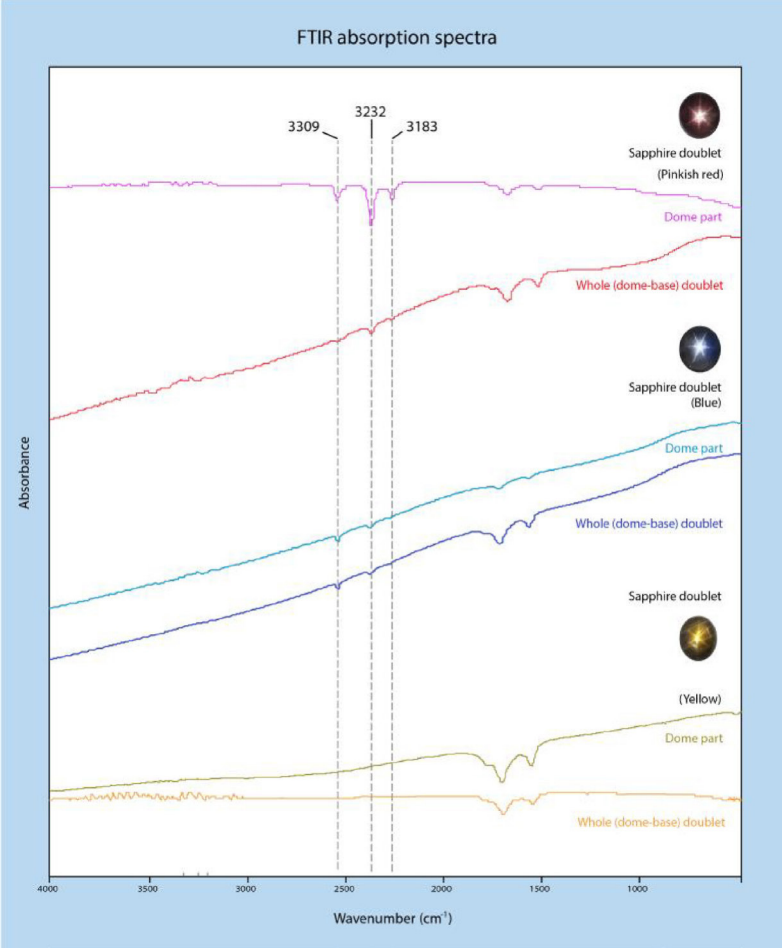

Figure 10 : Top two lines: FTIR spectra of the dome part (purple line) and the whole (dome+base) doublet (red line) of the pinkish red sample.

Middle two lines: FTIR spectra of the dome part (light blue line) and the whole (dome+base) doublet (blue line) of the blue sample.

Bottom two lines: FTIR spectra of the dome part (brown line) and the whole (dome+base) doublet (yellow line) of the yellow sample.

UV-Visible spectroscopic analysis

The non-polarized UV-Vis-NIR absorption spectrum of the dome part of the pinkish-red sample (Figure 11, upper) displayed broad absorption bands peaked at ~570 nm due to V and Cr transition (Krzemnicki, 2019) that is consistent with the chemical data by EDXRF. Such V/Cr related absorption band has given rise to the stone's pinkish-red coloration.

The non-polarized UV-Vis-NIR absorption spectrum of the dome part of the blue sample (Figure 11, middle) displayed broad absorption bands at ~500-840 nm as the result of Fe^{2+}/ Ti^{4+} inter-valence charge transfer (IVCT) mechanism (Lehmann and Harder, 1970; Krebs and Maisch, 1971; Pisutha-Arnond *et al*., 2019) and responsible for the blue coloration. Again the Fe^{2+}/ Ti^{4+} IVCT is consistent with the chemical data.

The non-polarized UV-Vis-NIR absorption spectra of the dome part of the yellow sample (Figure 11, lower) show the increasing absorption toward UV range due to color center (Schmetzer *et al*., 2004) that could be related to Ni (Thomas *et al*., 1997) and Fe shown in the chemical data.

Furthermore, the spectra of the whole (dome+base) doublet of all samples displayed an additional Fe^{3+} related absorption peak at 450 nm due to the natural sapphire base superimposed.

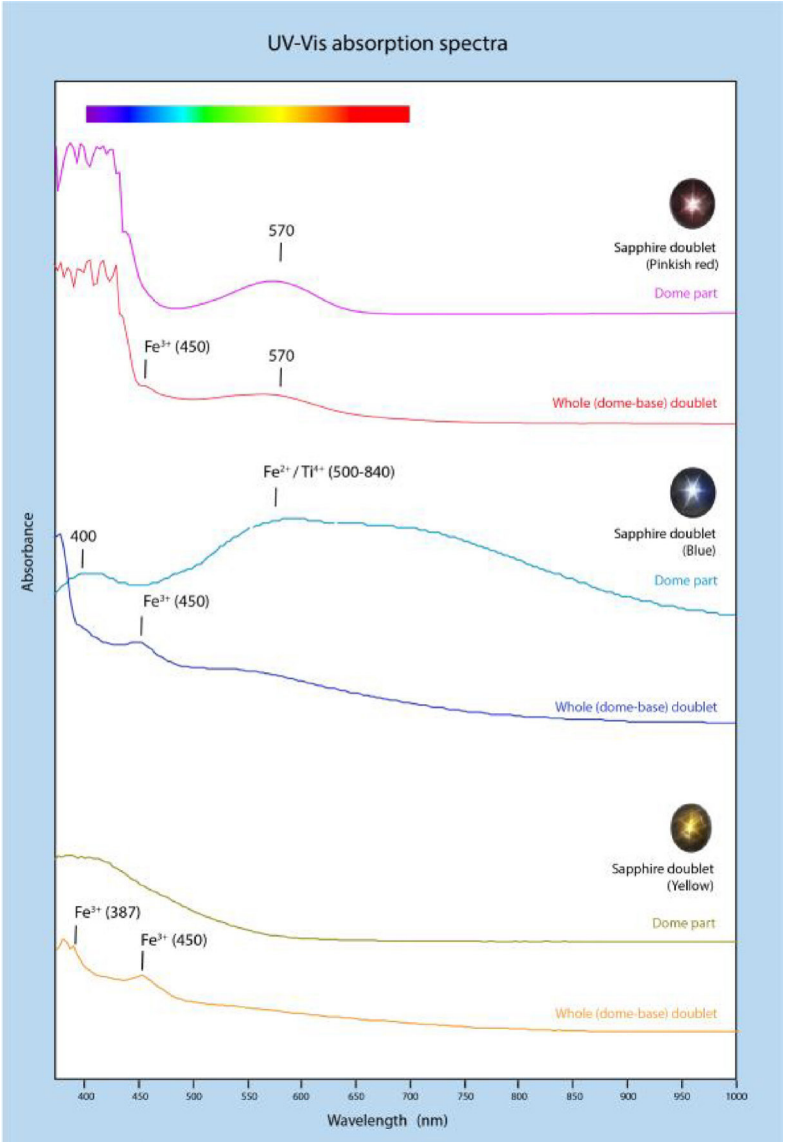

Figure 11 :
Top two lines: *UV-Vis-NIR spectra of the dome part (purple line) and the whole (dome+base) doublet (red line) of the pinkish red sample.*
Middle two lines: *UV-Vis-NIR spectra of the dome part (light blue) and the whole (dome+base) doublet (blue line) of the blue sample.*
Bottom two lines: *UV-Vis-NIR spectra of the dome part (brown line) and the whole (dome+base) doublet (yellow line) of the yellow sample.*

Summary and conclusion

In summary, all three pinkish-red, blue and yellow star stones are sapphire doublets composed of transparent synthetic sapphire dome top firmly glued (using a type of polymer) to a (low quality) natural black star sapphire base which is responsible for the star effect. The contact layer can easily be observed from the side view slightly below the stone's girdle by naked eye, loupe and microscope. Their standard gemological properties are: RI ~1.76 (spot reading), SG 3.98-4.05; Fluorescence: moderate chalky orange in SWUV and inert in LWUV for the pinkish-red stone, chalky blue along curved striation in SWUV and inert in LWUV for the blue stone, very weak red in both SWUV and LWUV for the yellow stone. Microscopic features: tiny gas bubbles, curved striation, or curved color banding in the dome pieces, dense piece, many trapped gas bubbles along the contact plane, fine silk inclusions along straight and angular growth zones in the base.

Advanced instruments were also used to confirm the stone identity. The Raman spectroscopy revealed the exposed adhesive substance at the contact plane to be a type of polymer. X-radiographs showed the presence of a heavy element in the glassy material in fractures of the base piece of the pinkish-red sample suggesting (in combination with chemical data) a lead-containing glass filler. The UV-Vis-NIR spectra of the pinkish-red sample displayed broad absorption bands peaked at ~570 nm due to V and Cr transition, giving rise to the pinkish-red coloration. The UV-Vis-NIR spectra of the blue sample showed broad absorption bands at~500-940 nm due to Fe^{2+}/ Ti^{4+} IVCT mechanism and responsible for the blue coloration. The UV-Vis-NIR spectra of the yellow sample showed the absorption due to color center that could relate to Ni and Fe. The chromophore elements in all three stones are consistent with the chemical data by EDXRF

In conclusion, these three samples can be called composite star sapphire doublet (see illustrate in Figure 12) that are assembled from transparent synthetic corundum (dome part) with a thin layer of (low quality) black star sapphire (base part).

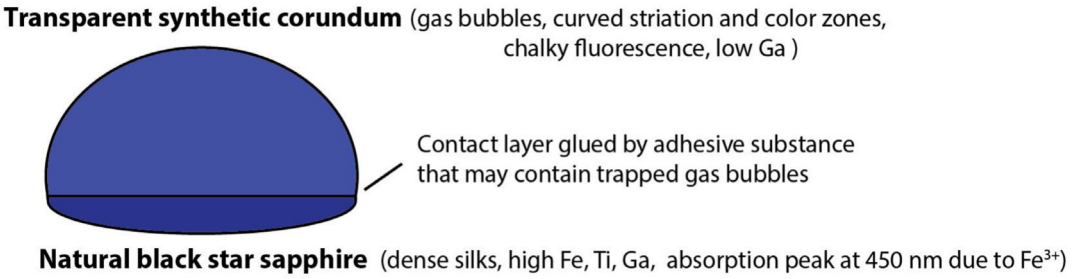

Figure 12 : The illustration from side view of these three samples showing explanation of composite corundum (synthetic corundum-natural black star sapphire doublet).

Acknowledgements

The authors would like to express our thanks to Mr. Thanong Leelawatanasuk, Dr. Visut Pisutha-Arnond, Mrs. Wilawan Atichat and Professor Dr. Chakkaphan Sutthirat for their valuable suggestions and kindly reviewing this article.

References :

Hughes R. W., Hughes E. B., Manorotkul W. (2020) Black star sapphire with dual treatments. *Gems & Gemology,* Vol. 56, No. 3, pp. 442-443. https://www.gia.edu/gems-gemology/fall-2020-gemnews-black-star-sapphire

Krebs J. J., Maisch W. G. (1971) Exchange effects in the optical-absorption spectrum of Fe^{3+} in Al_2O_3. *Physical Review B,* Vol. 4, No. 3, pp. 757.

Krzemnicki M. S. (2019) Vanadium – rich Ruby from Mogok, Myanmar, SSEF Facette, 25. https://www.ssef.ch/vanadium-rich-ruby-from-mogok-myanmar/

Leelawatanasuk T., Narudeesombat N., Saengbuangamlam S., Lhuaamporn T. (2014) Golden Sheen and Non-Sheen Sapphire from Kenya. *Proceedings of the 4th International Gem and Jewelry Conference (GIT2014)*, Bangkok, https://www.git.or.th/eng/testing_center_en/lab_notes_en/glab_en/2016/11/D5-A0210-1.pdf

Lehmann G., Harder H. (1970) Optical spectra of di-and trivalent iron in corundum. *American Mineralogist*, Vol. 55, No. 1-2, pp. 98-105.

Mayerson W. M. (2003) Lab Notes: Sapphire/Synthetic color-change sapphire doublets. *Gems & Gemmology*, Vol. 49,, No. 2, pp. 149-150.

Muhlmeister S., Fritsch E., Shigley J. E., Devouard B., Laurs B. M. (1998) Separating Natural and Synthetic Rubies on The Basis of Trace – Element Chemistry. *Gems & Gemology,* Vol. 34, No. 2, pp. 80-101, https://www.gia.edu/doc/Separating-Natural-and-Synthetic-Rubies-on- the-Basis-of-Trace-Element-Chemistry.pdf

Pisutha-Arnond V., Promwongnan S., Narudeesombat N., Ounorn P., Leelawatanasuk T., Sripoonjan T., Nilhud N., Atichat W. (2019) Blue diffusion-treated natural & synthetic sapphires recently available in the market. *Journal of the Gemmological Association of Hong Kong*, Vol. 40, pp. 87-95, https://www.git.or.th/eng/testing center_en/lab_notes_en/glab_en/2019/10/Doc-26102019.pdf

Promwongnan S., Leelawatanasuk T., Saengbuangamlam S. (2016) *A lead-glass-filled corundum doublet. Journal of Gemmology,* Vol. 35, No. 1, pp. 64-68, http://dx.doi.org/10.15506/JoG.2016.35.1.64.

References :

Schmetzer K., Schwarz D. (2004) The causes of colour in untreated, heat treated and diffusion treated orange and pinkish-orange sapphires - a review. *Journal of Gemmology*, Vol. 29, No. 3, pp. 149-182.

Sehgal A. (2016) Lab Notes: Lead glass-filled black star sapphire. *Gems & Gemmology*, Vol. 52, No. 3, pp. 304-305

Smith C. P. (1995) A contribution to understanding the infrared spectra of rubies from Mong Hsu, Myanmar. *Journal of Gemmology*, Vol. 24, No. 5, pp. 321-335.

Thomas V. G., Mashkovtsev R. I., Smirnov S. Z., Maltsev V. S. (1997) Tairus hydrothermal synthetic sapphires doped with nickel and chromium. *Gems & Gemology*, Vol. 33, No. 3, pp. 188-202.